

## ORIGINAL ARTICLE

# Mechanical properties of a polymer network of Tetra-PEG gel

Asumi Sugimura<sup>1</sup>, Makoto Asai<sup>1</sup>, Takuro Matsunaga<sup>1</sup>, Yuki Akagi<sup>2</sup>, Takamasa Sakai<sup>2</sup>, Hiroshi Noguchi<sup>1</sup> and Mitsuhiro Shibayama<sup>1</sup>

The elastic properties of Tetra-polyethylene glycol (PEG) gel, a four-armed PEG network gel, were studied by simulating the deformation of elastic networks containing defects that are randomly introduced to the network. This network model accurately reproduced the experimental results observed for Tetra-PEG gel. In particular, the stress-extension ratio curve of the gel prepared at chain-overlap concentration was in agreement with that of a regular network without defects. As the defect density increased, the Young's modulus decreased linearly. The fracture and spatial inhomogeneity of the networks were also investigated in the simulation.

*Polymer Journal* (2013) 45, 300–306; doi:10.1038/pj.2012.149; published online 15 August 2012

**Keywords:** defect gel; large deformation; percolation; polymer gel; Tetra-PEG gel

## INTRODUCTION

Polymer gels are defined as polymer networks that swell in water (hydrogels), oil (lipogels) or air (aerogels). Owing to their high water-retention properties and flexibility, polymer gels are used as super absorbents, oil-recovery materials and mechanical absorbers. However, their mechanical fragility limits their application in structural materials. In particular, applications in biomedical materials such as artificial muscle, cartilage and tendons, which have been desired for many years, are not yet possible because muscular and tendinous systems require materials with both mechanical properties and biocompatibility.<sup>1–3</sup>

It is well known that the mechanical fragility of polymer gels is caused by the spatial structural inhomogeneity of the polymer network.<sup>4–9</sup> This inhomogeneity is formed by spatial fluctuations in the concentration of monomer and/or the crosslinking agent during the gelation process. Moreover, when entanglements and/or loops exist in the network, the network becomes topologically inhomogeneous, causing spatial structural inhomogeneity. To realize an ideal polymer network, many researchers have attempted to prepare 'model networks' using asymmetrical combinations of monodispersed multifunctional polymer and low-molecular-weight crosslinkers.<sup>10–13</sup> However, small-angle neutron scattering and sol fraction measurements have shown that the obtained polymer networks contain significant inhomogeneities.<sup>14–17</sup> Recently, several novel gels with advanced mechanical properties based on markedly different concepts were proposed: namely, slide ring gels,<sup>18</sup> nanocomposite gels<sup>19</sup> and double network gels.<sup>20</sup> In 2008, Sakai *et al.*<sup>21</sup> developed four-arm polyethylene glycol (PEG) gels, which are

biocompatible and easy to fabricate. The Tetra-PEG gel consists of two kinds of four-arm PEG macromers of the same size: tetra-amine-terminated PEG (TAPEG) and tetra-*N*-hydroxysuccinimide-glutarate-terminated PEG (TNPEG). Tetra-PEG gel has incredible mechanical strength: when a compressive strain over 90% is applied to Tetra-PEG gel, it can return to its original form without hysteresis. The rupture strength of Tetra-PEG gels can reach tens of MPa, which is equal to that of a human cartilage (6–10 MPa).<sup>22</sup> Hence, Tetra-PEG gel is expected to be applicable as biomedical materials. The small-angle neutron scattering result showed that practically no spatial inhomogeneities exist.<sup>22</sup> Furthermore, the inhomogeneities did not appear even under the equilibrium swelling condition,<sup>23</sup> where spatial inhomogeneities are known to become apparent in other polymer gels.<sup>24–26</sup>

In this paper, we investigated by computer simulation the mechanical behavior of the Tetra-PEG gel at a large deformation regime. We represented the Tetra-PEG gel as a network of elastic bonds. The networks of harmonic bonds or inextensible bonds<sup>27</sup> have been used to study the mechanical properties of gels. As Tetra-PEG gels exhibit large deformation, the nonlinearity of the bonds can have a role. Therefore, we develop a network model of worm-like chains (WLC), which takes into account the finite length of polymer chains, and we study the large deformation of the gels. To investigate the relationship between spatial structural inhomogeneity and mechanical properties of gels, we introduce 'defects' into the polymer network by randomly cutting the network chains. With this method, we can evaluate the extent of spatial structural inhomogeneity and discuss the relationship between spatial structural inhomogeneity and mechanical properties.

<sup>1</sup>Institute for Solid State Physics, The University of Tokyo, Kashiwa, Chiba, Japan and <sup>2</sup>Department of Bioengineering, School of Engineering, The University of Tokyo, Bunkyo-ku, Tokyo, Japan

Correspondence: Professor M Shibayama, Institute for Solid State Physics, The University of Tokyo, 5-1-5 Kashiwanoha, Kashiwa, Chiba 277-8581, Japan.

E-mail: sibayama@issp.u-tokyo.ac.jp

Received 16 January 2012; revised 31 May 2012; accepted 13 June 2012; published online 15 August 2012

## EXPERIMENTAL PROCEDURE

TAPEG and TNPEG were prepared from tetrahydroxyl-terminated PEG with equal arm lengths. The details of TAPEG and TNPEG preparation were reported previously.<sup>22</sup> The molecular weights ( $M_w$ ) of TAPEG and TNPEG were matched with each other ( $M_w = 10 \text{ kg mol}^{-1}$ ). The activity of the functional group was estimated using nuclear magnetic resonance. Tetra-PEG gels were synthesized as follows. Equal amounts of TAPEG and TNPEG ( $40\text{--}140 \text{ mg ml}^{-1}$ ) were dissolved in phosphate buffer (pH 7.4) and phosphate-citric acid buffer (pH 5.8), respectively. The corresponding initial polymer volume fractions,  $\phi_0$ , ranged from  $3.54 \times 10^{-2}$  to  $1.24 \times 10^{-1}$  (mass density =  $1.129 \text{ g cm}^{-3}$ ). To control the reaction rate, the ionic strengths of the buffers were chosen to be 25 mM for the lower macromer concentrations ( $40\text{--}80 \text{ mg ml}^{-1}$ ) and 50 mM for the higher macromer concentrations ( $100\text{--}140 \text{ mg ml}^{-1}$ ). The two solutions were mixed, and the resultant solution was poured into the mold. At least 12 h was allowed for reaction completion before performing stretching measurements on dumbbell-shaped films using a mechanical testing apparatus (CR-500DX-SII rheometer; Sun Scientific Co., Tokyo, Japan) at a crosshead speed of  $0.1 \text{ mm s}^{-1}$ .

## Network model and simulation method

A gel is modeled with a network of elastic bonds. First, we construct a regular network on a diamond lattice, where each node (crosslink point) has four bonds with length  $l_0$  (see Figure 1a). When a Tetra-PEG gel is formed without any defects, the gel is considered to have this diamond lattice structure. The periodic boundary condition is used. The total number of nodes and bonds are  $N_{\text{node}} = 8000$  and  $N_{\text{bond}} = 16000$ , respectively. To investigate the effects of inhomogeneity, bond defects are introduced by random removal of the bonds. For a diamond lattice, the network is percolated for the ratio of left bonds  $P \geq 0.39$ .<sup>28</sup> We varied the bond ratio from  $P = 0.45$  to 1 in this work.

The  $i$ -th elastic bond is represented by WLC potential,

$$U_b(r_i) = \frac{k_B T r_i^2}{4l_p l_{\text{max}}} \left( \frac{3l_{\text{max}} - 2r_i}{l_{\text{max}} - r_i} \right) \quad (1)$$

$$\mathbf{f}_b(\mathbf{r}_i) = \frac{k_B T}{l_p} \left\{ \frac{r_i}{l_{\text{max}}} + \frac{1}{4} \left( \frac{1}{(1 - r_i/l_{\text{max}})^2} - 1 \right) \right\} \frac{\mathbf{r}_i}{r_i} \quad (2)$$

where  $l_{\text{max}}$  and  $l_p$  are the contour and the persistence lengths of the bond chain, respectively. The total energy is  $U = \sum_i U_b(r_i)$ , and  $k_B T$  is the thermal energy. For  $r_i \ll l_{\text{max}}$ , the force follows Hooke's law:  $\mathbf{f}_{\text{WLC}}(\mathbf{r}_i) = (3k_B T / 2l_p l_{\text{max}}) \mathbf{r}_i$ , while  $\mathbf{f}_{\text{WLC}}(\mathbf{r}_i) \rightarrow \infty$  at  $r_i \rightarrow l_{\text{max}}$ . This potential reproduces the force acting on the stretched DNA or polystyrene very well.<sup>29–31</sup> Here,  $l_{\text{max}} = 40$ ,  $l_p = 1.1$  and  $l_0 = 5.6 \text{ nm}$  are used to represent a Tetra-PEG gel made from 10-kDa macromonomers.

To measure the stress-extension ratio curve of the gel, the gel is gradually stretched by the change of the aspect ratio of the simulation box with constant volume  $V = L_x L_y L_z$ :  $L_x = \lambda L_0$ ,  $L_y = L_z = \lambda^{-1/2} L_0$ , where  $L_0$  is the side length of the initial cubic simulation box. As the lattice structure is symmetric, no difference is seen among the stretching in the  $x$ ,  $y$  and  $z$  directions. After a small change of the ratio  $\lambda$  in each direction, the gel network is relaxed to the equilibrium state. The position of the  $n$ -th node is moved by the equation

$$\eta \frac{d\mathbf{r}_n}{dt} = \mathbf{f}_n \quad (3)$$

where  $\mathbf{f}_n = -\partial U / \partial \mathbf{r}_n$ . Equation (3) is numerically solved using the Euler method as  $\mathbf{r}_n(t + \Delta t) = \mathbf{r}_n(t) + \mathbf{f}_n \Delta t / \eta$  until  $|U(t + \Delta t) - U(t)| / U(t) < 10^{-9}$ . The time step  $\Delta t / \eta$  is adjusted to keep  $U(t + \Delta t) \leq U(t)$ . The breaking extension is defined as 95% of  $l_{\text{max}}$ . If a bond between two nodes is broken, the two nodes do not interact with each other. The computation scheme is shown in Figure 2.

## RESULTS AND DISCUSSION

The stress-extension ratio curve is investigated for various bond ratios  $P$ . The nominal stress is calculated from the stress tensor:  $\sigma = \{P_{xx} - (P_{yy} + P_{zz})/2\} / \lambda$ , with  $P_{\alpha\alpha} = L_0^{-3} \{m v_{n,\alpha}^2 + \sum_i^{N_{\text{bond}}} r_{i,\alpha} f_{b,\alpha}(\mathbf{r}_i)\}$ , where  $\alpha \in \{x, y, z\}$  and  $m$  is the mass of the node. As the thermal fluctuations are neglected here, the kinetic term vanishes ( $v^2 = 0$ ). The curves with circles in Figures 3a and b show the stress-extension ratio

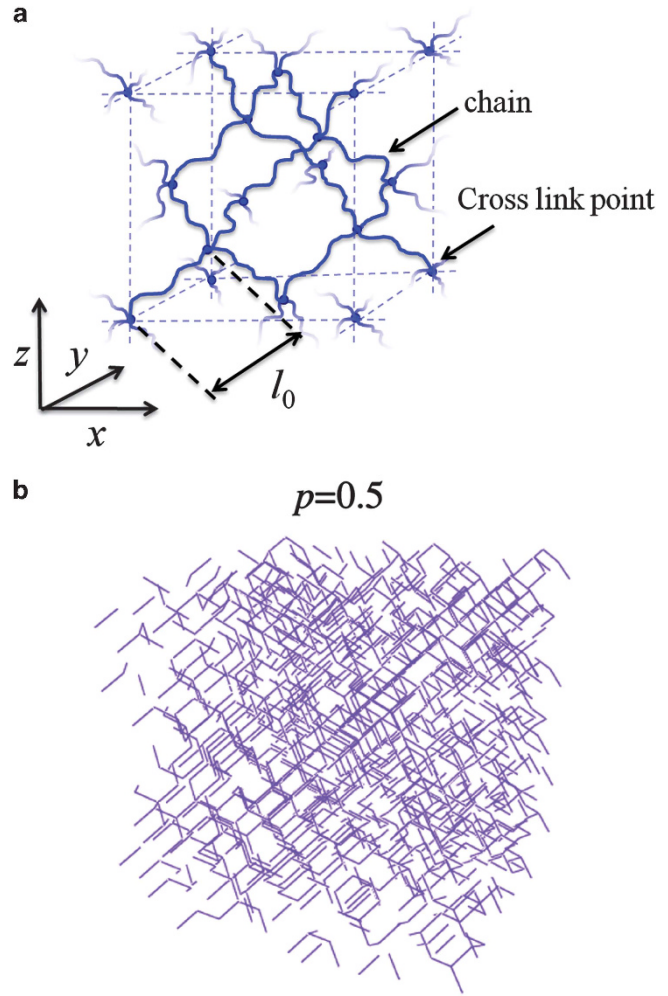


**Figure 1** Structure of an elastic network. (a) Structure of an elastic network on a diamond lattice. (b) Structure of the diamond lattice at  $P = 0.5$ .

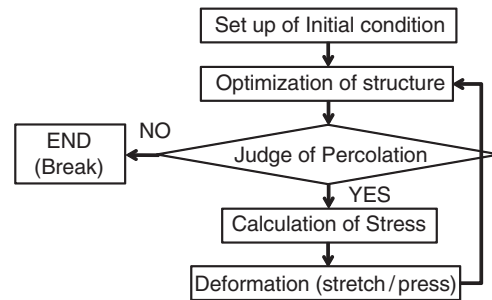


**Figure 2** Computation scheme.

curves for stretched and compressed gels without defects ( $P = 1$ ), respectively. These curves accurately reproduce the stress-extension ratio curves of the 10k-Tetra-PEG gel at 6 wt% (the curves with the + marks) well. This agreement indicates that this Tetra-PEG gel forms a regular polymer network with defects. The deviation for highly compressed gels shown in Figure 3b would be caused by the excluded volume effects, which are neglected in the simulations. For

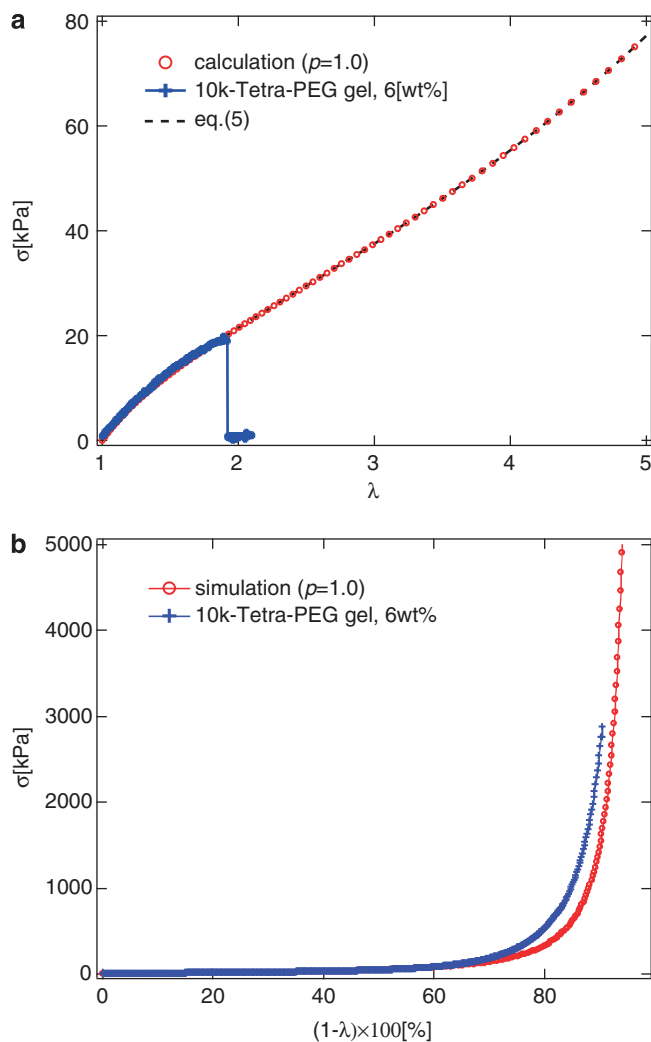


**Figure 3** Stress-extension ratio curve for (a) stretching and (b) compression of gels.

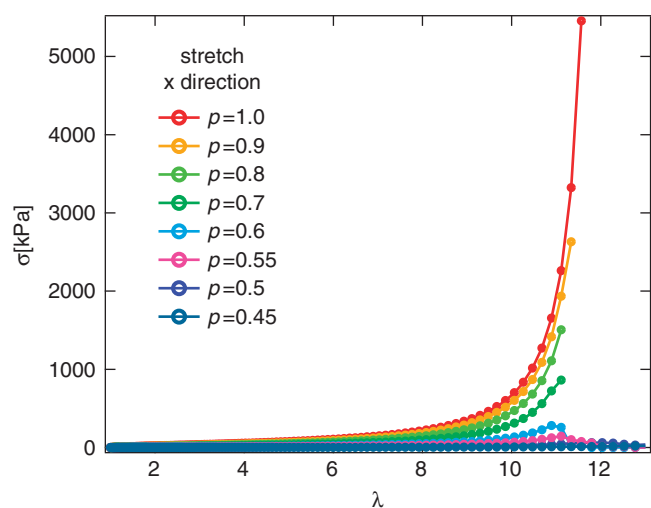


**Figure 4** Stress-extension ratio curve for stretching of the gel at various bond ratios  $P$ .

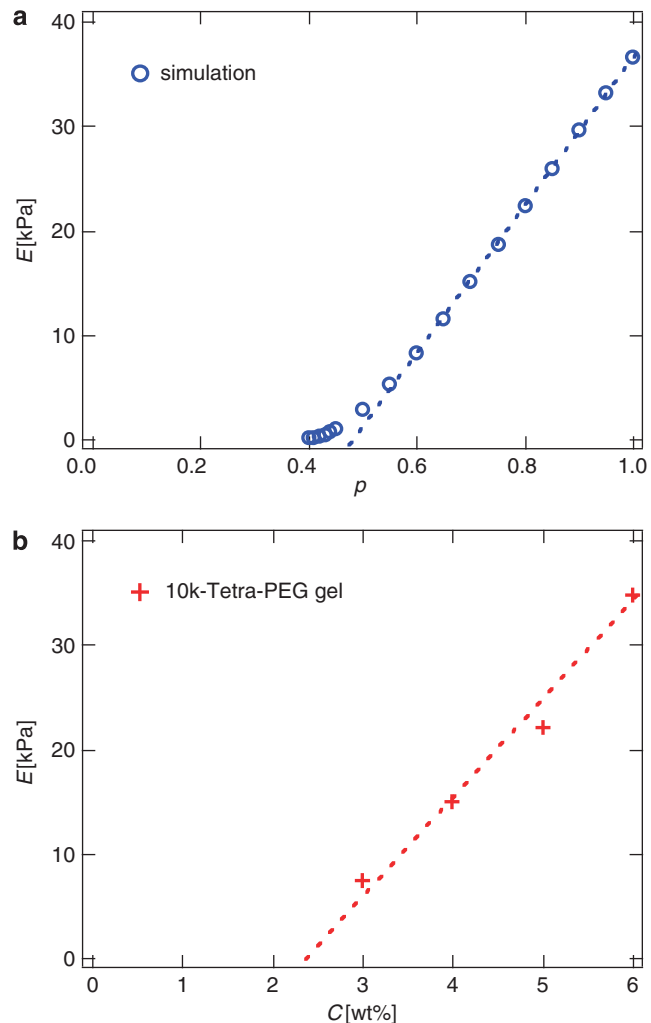


**Figure 5** Dependence of Young's modulus  $E$  on (a) the bond ratio  $P$  in the simulation and (b) the concentration  $C$  of the 10-k Tetra-PEG gel.

$|\lambda-1| \ll 1$ , the polymer chains between the crosslink points are considered ideal, and the nominal stress is proportional to the chain density ( $N/V$ ) as follows:

$$\sigma \propto \frac{Nk_B T}{V} \left( \lambda - \frac{1}{\lambda^2} \right) \quad (4)$$

where  $N$  and  $V$  are the number of effective chains and the volume, respectively. As Tetra-PEG gels withstand much greater deformation than that described by Equation (4), the nonlinear elasticity of the polymer chains must be taken into account. When the WLC-chain network of a cubic lattice is assumed, the nominal stress is given by:

$$\sigma = \frac{Nk_B T}{3V} \left[ \left( \lambda - \frac{1}{\lambda^2} \right) \frac{l_0^2}{l_{\max} l_p} + \frac{l_0}{4l_p} \left\{ \left( 1 - \frac{\lambda l_0}{l_{\max}} \right)^{-2} - \lambda^{-\frac{3}{2}} \left( 1 - \frac{l_0}{\lambda^{1/2} l_{\max}} \right)^{-2} - \left( 1 - \frac{1}{\lambda^{3/2}} \right) \right\} \right] \quad (5)$$

The stretching of the elastic networks at  $P=1$  and of the Tetra-PEG gels is well explained by Equation (5), as shown in Figure 3a.

As the defects of the networks increase ( $P$  decreases), the stretching force decreases as shown in Figure 4. When the gel network chains can rearrange their relative positions at low  $P$ , two non-neighbor

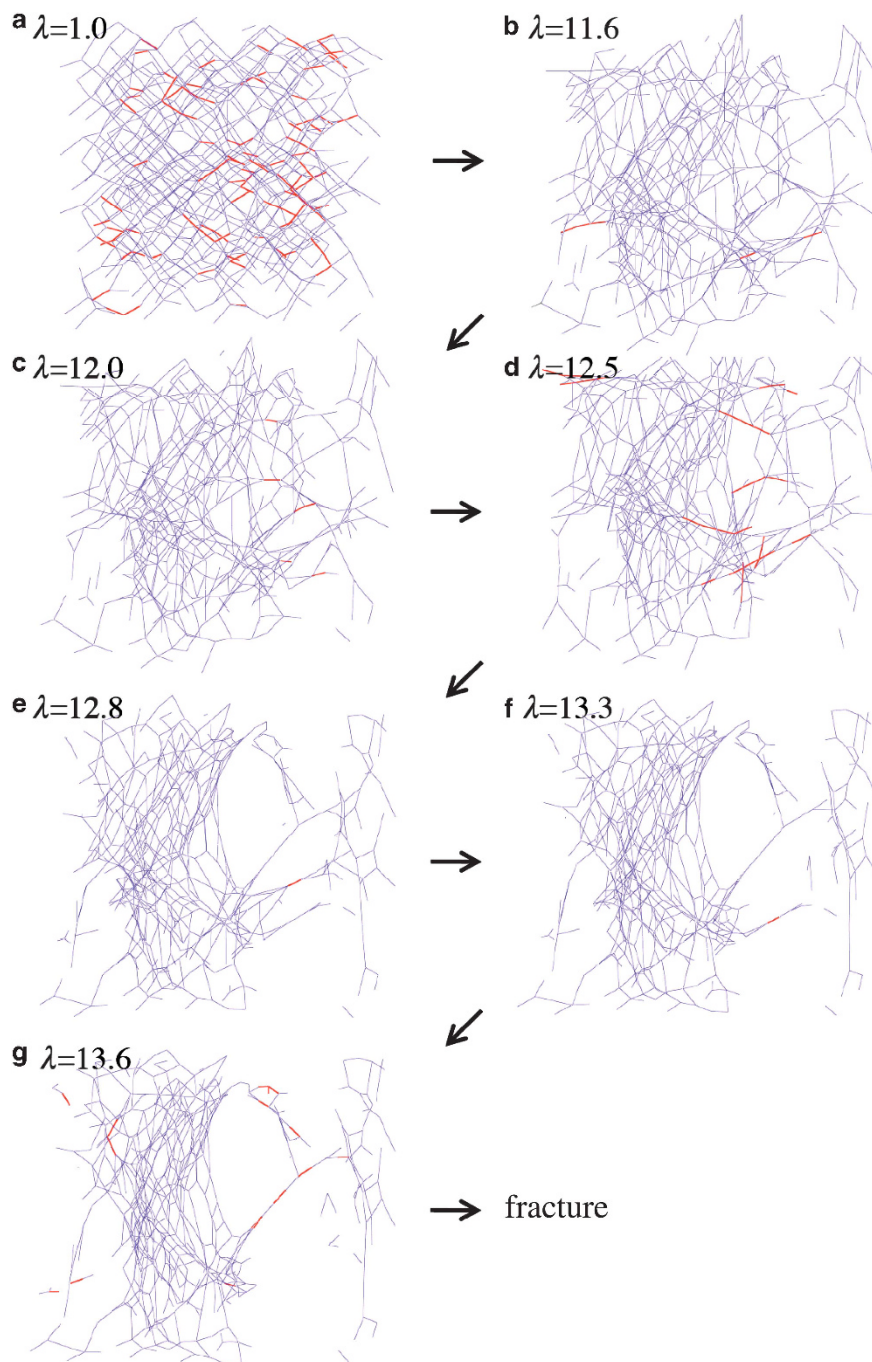


**Figure 6** Sequential snapshots of the fracture dynamics of the gel network at different extension ratios,  $\lambda$ , (a)  $\lambda = 1.0$  to (g)  $\lambda = 13.6$ , where  $\lambda$  is extension ratio in  $x$  direction. The bond ratio,  $P$ , is 0.9. The blue lines represent polymer chains, and red lines represent bonds broken during the stretch to the next snapshot. In this case, fracture occurs when  $\lambda$  becomes greater than 13.6.

crosslink points often connect with straight bonds. These short connections progressively reduce the local stress.

The Young's modulus of obtained gels  $E$  is shown in Figure 5a. Except for the region near the percolation transition ratio  $P_c = 0.39$ ,  $E$  is linearly dependent on  $P$ . The experimental result of the relationship between  $E$  and the concentration  $C$  of Tetra-PEG gel is shown in Figure 5b. We measured  $E$  at  $C = 3.0\text{--}6.0$  wt%. The Tetra-PEG gels show a similar linear dependence on  $C$ , which suggests that the

defects of Tetra-PEG gels increase with a decrease in  $C$ . Thus, the defect density can be controlled by the concentration of the initial macromonomers.

Figures 6 and 7 show the fracture dynamics of the gel network at  $P = 0.9$ . In Figure 6, the breakup of the polymer chains does not occur homogeneously in the gel. A clear fracture surface is seen in Figure 7. The red dots mark the break points. Therefore, the region that is thick that contains a high density of dots indicates a fracture

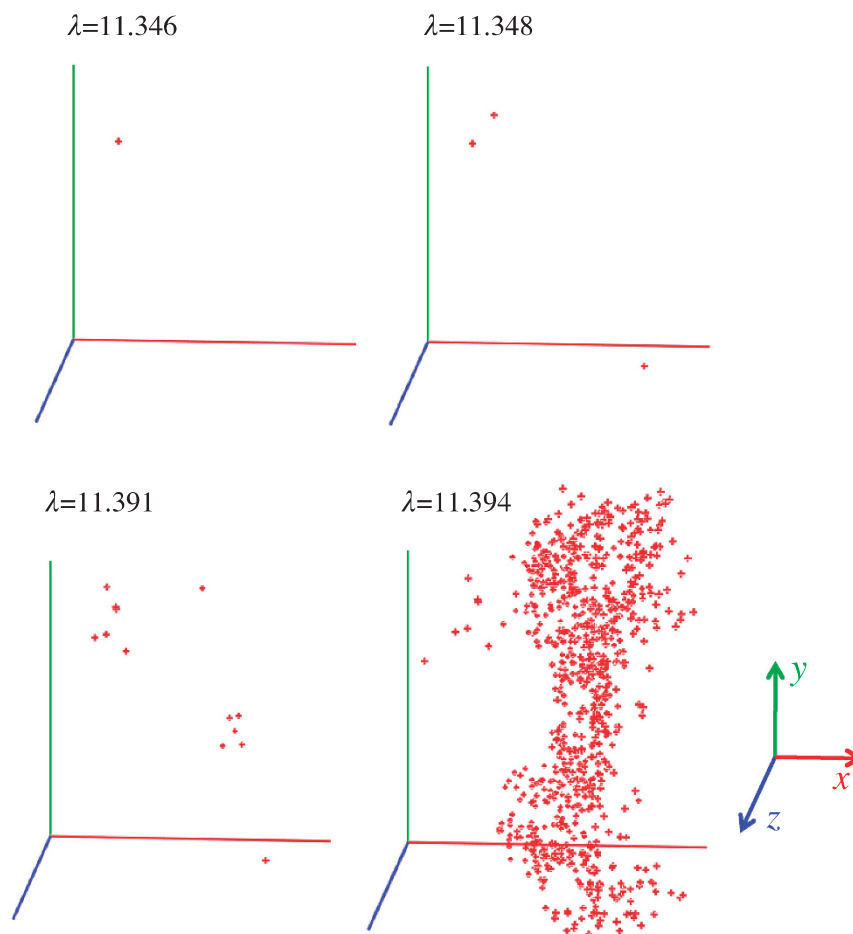


**Figure 7** Broken bonds for the gel fracture at  $P=0.9$ . The center positions of the broken bonds are shown in the normalized coordinates ( $x/L_x, y/L_y, z/L_z$ ).

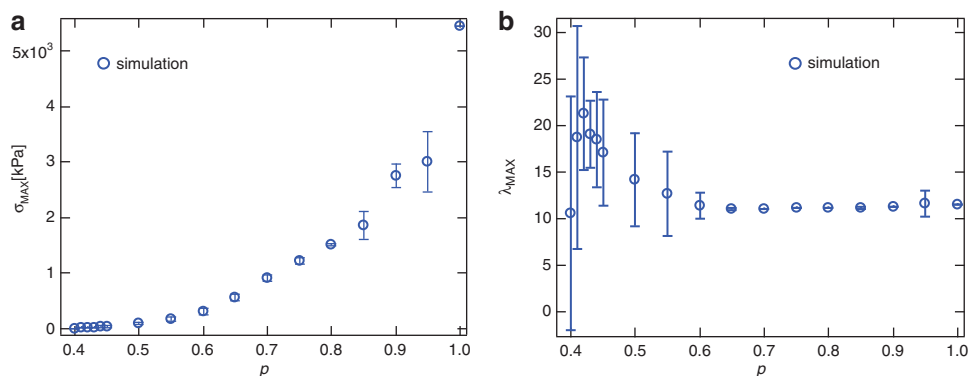


**Figure 8** Dependence of the bond ratio  $P$  on (a) the bond-breakup stress  $\sigma_{\max}$  and (b) extension ratio  $\lambda_{\max}$ .

surface. When a chain is broken, the neighboring chains are exposed to additional local stress forces, which lead to another chain breakup.

Figures 8a and b show the stress and extension ratio at break, respectively. At lower  $P$ , the fracture of the gels occurs at lower stress. By contrast, the extension ratio decreases with increasing  $P$  and is almost constant for  $P > 0.6$ . This stress dependence can be explained by the length distribution of the polymer chains shown in Figure 9.

When the gels have a few defects, the polymer chains have a uniform length during the stretching, so the gel has high fracture stress. With decreasing  $P$ , the fraction of 'short' chains increases. At  $P = 0.45$ , most chains are short, and a few chains are highly stretched because of the inhomogeneity of the network. As the total stretching force is balanced with a few percolated polymer chains, the chains break with a small amount of stretching. Thus, homogeneity of the network is significant for preventing gel fracture.

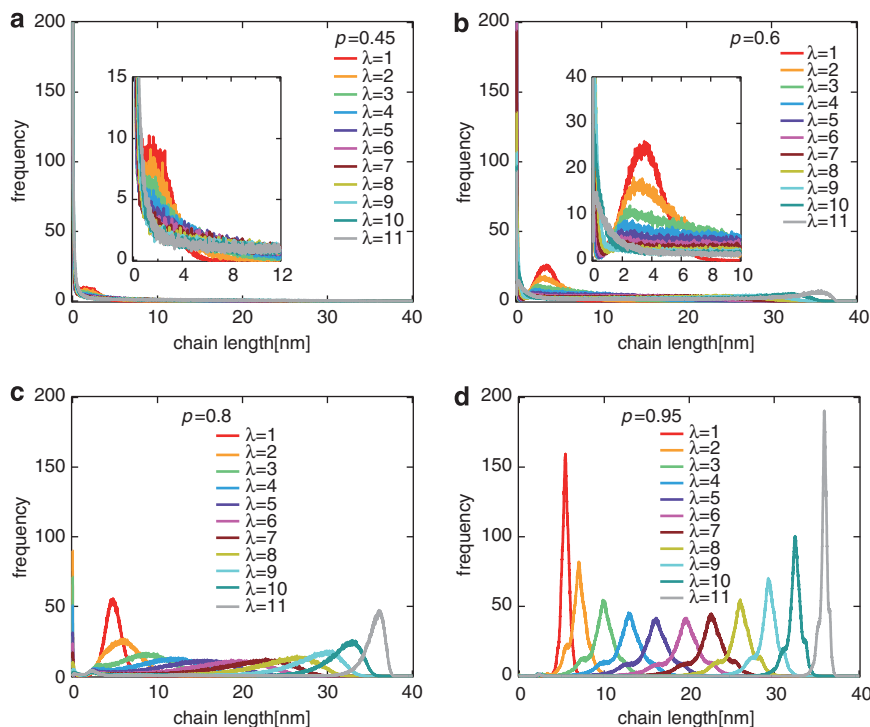


**Figure 9** Length distribution of the elastic bonds of stretched gels at  $P=$  (a) 0.45, (b) 0.6, (c) 0.8 and (d) 0.95.

We also investigate the effects of thermal fluctuations using the underdamped Langevin equation instead of Equation (3) as follows,

$$m \frac{d\mathbf{v}_n}{dt} = \mathbf{f}_n - \eta \mathbf{v}_n + \mathbf{g}_n \quad (6)$$

where  $\mathbf{g}_n$  denotes the random forces modeled as Gaussian white noise:

$$\langle g_{nz}(t) g_{n\beta}(t') \rangle = 2\eta k_B T \delta_{nm} \delta_{z\beta} (t - t') \quad (7)$$

The Langevin equation is integrated by the leapfrog algorithm with  $m = \eta \tau_0$  and a time unit  $\tau_0 = \eta l_0^2 / k_B T$ . Although the resultant stress increases slightly, no significant difference is obtained (data not shown). The thermal fluctuations of the crosslink positions are not important for determining the gel elasticity.

## CONCLUDING REMARKS

We studied the elastic properties of Tetra-PEG gel by simulating elastic networks with a diamond lattice. We find that the 10-k-Tetra-PEG gel at 6.0 wt% can be considered to have a regular diamond network with a few defects. As the polymer concentration  $C$  decreases, the Young's modulus of the Tetra-PEG gels linearly decreases. This decrease is interpreted as an increase in defects in the network. Thus, our network model reproduces the experimental results of Tetra-PEG gel well.

We also investigated the fracturing of the gel. The fracture stress decreases with increasing defects in the network, whereas the fracture extension ratio is much less dependent on the defect density. The gels become fragile as the networks become inhomogeneous. Thus, homogeneity of the gels is important for strong gels such as Tetra-PEG gel.

## ACKNOWLEDGEMENTS

This work has been financially supported by Grant-in-Aids for Scientific Research from the Ministry of Education, Culture, Sports, Science and Technology (no. 22245018 to MS).

- Martens, P. & Anseth, K. S. Characterization of hydrogels formed from acrylate modified poly(vinyl alcohol) macromers. *Polymer* **41**, 7715–7722 (2000).
- Lutolf, M. P. & Hubbell, J. A. Synthesis and physicochemical characterization of end-linked poly(ethylene glycol)-co-peptide hydrogels formed by michael-type addition. *Biomacromolecules* **4**, 713–722 (2003).
- Azab, A. K., Orkin, B., Doviner, V., Nissan, A., Klein, M., Srebnik, M. & Rubinstein, A. Crosslinked chitosan implants as potential degradable devices for brachytherapy: *in vitro* and *in vivo* analysis. *J. Control. Release* **111**, 281–289 (2006).
- Stein, R. S. The determination of the inhomogeneity of crosslinking of a rubber by light scattering. *J. Polym. Sci.* **7**, 657–660 (1969).
- Pines, E. & Prins, W. The effect of nonrandom crosslinking on the light scattering of swollen polymer networks. *J. Polym. Sci., Polym. Phys. Polym. Lett.* **10**, 719–724 (1972).
- Candau, S., Bastide, J. & Delsanti, M. Structural, elastic, and dynamic properties of swollen polymer networks. *Adv. Polym. Sci.* **44**, 27–71 (1982).
- Panyukov, S. & Rabin, Y. Polymer gels: frozen inhomogeneities and density fluctuations. *Macromolecules* **29**, 7960–7975 (1996).
- Bastide, J. & Candau, S. J. Structure of gels as investigated by means of static scattering techniques. (Chapter 9). In *The Physical Properties of Polymer Gels*. Addad, J.P. Ed. (John Wiley, New York 143, 1996).
- Shibayama, M. Spatial inhomogeneity and dynamic fluctuations of polymer gels. *Macromol. Chem. Phys.* **199**, 1–30 (1998).
- Dusek, K. The role of precursor architecture in polymer network structure. *Trends Polym. Sci.* **5**, 268–274 (1997).
- Hild, G. Model networks based on 'endlinking' processes: synthesis, structure and properties. *Prog. Polym. Sci.* **23**, 1019–1149 (1998).
- Malkoch, M., Vestberg, R., Gupta, N., Mespouille, L., Dubois, P., Mason, A. F., Hedrick, J. L., Liao, Q., Frank, C. W., Kingsbury, K. & Hawker, C. Synthesis of well-defined hydrogel networks using Click chemistry. *J. Chem. Commun.* **26**, 2774–2776 (2006).
- Durackova, A., Valentova, H., Duskova-Smrckova, M. & Dusek, K. Effect of diluent on the gel point and mechanical properties of polyurethane networks. *Polym. Bull.* **58**, 201–211 (2007).
- Shibayama, M., Takahashi, H. & Nomura, S. Small-angle neutron scattering study on end-linked poly(tetrahydrofuran) networks. 1. Stoichiometrically cross-linked gels. *Macromolecules* **28**, 6860–6864 (1995).
- Villar, M. A. & Valles, E. M. Influence of pendant chains on mechanical properties of model poly(dimethylsiloxane) networks. 2. Viscoelastic properties. *Macromolecules* **29**, 4081–4089 (1996).
- Patel, S. K., Malone, S., Cohen, C., Gillmor, J. R. & Colby, R. H. Elastic modulus and equilibrium swelling of poly(dimethylsiloxane) networks. *Macromolecules* **25**, 5241–5251 (1992).
- Mendes, E., Girard, B., Picot, C., Buzier, M., Boue, F. & Bastide, J. Small-angle neutron scattering study of end-linked gels. *Macromolecules* **26**, 6873–6877 (1993).
- Okumura, Y. & Ito, K. The polyrotaxane gel: a topological gel by figure-of-eight crosslinks. *Adv. Mater.* **13**, 485–487 (2001).

- 19 Haraguchi, K. & Takehisa, T. Nanocomposite hydrogels: a unique organic–inorganic network structure with extraordinary mechanical, optical, and swelling/de-swelling properties. *Adv. Mater.* **14**, 1120–1124 (2002).
- 20 Gong, J. P., Katsuyama, Y., Kurokawa, T. & Osada, Y. Double-network hydrogels with extremely high mechanical strength. *Adv. Mater.* **15**, 1155–1158 (2003).
- 21 Sakai, T., Matsunaga, T., Yamamoto, Y., Ito, C., Yoshida, R., Suzuki, S., Sasaki, N., Shibayama, M. & Chung, U. I. Design and fabrication of a high-strength hydrogel with ideally homogeneous network structure from tetrahedron-like macromonomers. *Macromolecules* **41**, 5379–5384 (2008).
- 22 Matsunaga, T., Sakai, T., Akagi, Y., Chung, U. & Shibayama, M. Structure characterization of Tetra-PEG gel by small-angle neutron scattering. *Macromolecules* **42**, 1344–1351 (2009).
- 23 Matsunaga, T., Sakai, T., Akagi, Y., Chung, U. I. & Shibayama, M. SANS and SLS studies on Tetra-Arm PEG gels in as-prepared and swollen states. *Macromolecules* **42**, 6245–6252 (2009).
- 24 Bastide, J. & Leibler, L. Large-scale heterogeneities in randomly cross-linked networks. *Macromolecules* **21**, 2647–2649 (1988).
- 25 Mendes, E., Oeser, R., Hayes, C., Boue, F. & Bastide, J. Small-angle neutron scattering study of swollen elongated gels: butterfly patterns. *Macromolecules* **29**, 5574–5584 (1996).
- 26 Shibayama, M., Shirotani, Y. & Shiwa, Y. Static inhomogeneities and dynamics of swollen and reactor-batch polymer gels. *J. Chem. Phys.* **112**, 442–449 (2000).
- 27 Farago, O. & Kantor, Y. Entropic elasticity of two-dimensional self-avoiding percolation systems. *Phys. Rev. Lett.* **85**, 2533–2536 (2000).
- 28 Stauffer, D. & Aharony, A. *Introduction to Percolation Theory*. Taylor & Francis, 2nd ed., p. 17 (1994).
- 29 Marko, J. F. & Siggia, E. D. Stretching DNA. *Macromolecules* **28**, 8759–8770 (1995).
- 30 Bustamante, C. Entropic elasticity of lambda-phage DNA. *Science* **265**, 1599–1600 (1994).
- 31 Sakai, Y., Ikehara, T., Nishi, T., Nakajima, K. & Hara, M. Nanorheology measurement on a single polymer chain. *Appl. Phys. Lett.* **81**, 724–726 (2002).